Mass Transfer in a Sparged Contactor: Part I. Physical Mechanisms and Controlling Parameters

W. J. BRAULICK, J. R. FAIR, and B. J. LERNER

University of Texas, Austin, Texas

Studies of the air oxidation of aqueous sodium sulfite solutions were made in simple bubble contacting columns of 3-, 4-, and 6-in. diameter. Superficial gas rates up to 300 lb./hr.-sq.ft. were used. Contacting action is described in detail, and comparisons with air-water data show the marked influence of small, ionic bubbles. Mass transfer and dynamic gas holdup data are presented, and the former are compared with mass transfer data for bubble-cap trays.

This investigation was prompted by difficulties experienced in the initial operation in 1952 of a pilot plant for the production of acrylonitrile by reaction of acetylene and hydrocyanic acid in a liquid catalyst. While the early difficulties were rapidly resolved and the commercial plant has now been successfully operated for over ten years, these bubble reactor studies have only recently begun to assume wider importance, primarily because of increasing interest in liquid-phase oxidations.

Except for the excellent basic work of Shulman and Molstad (*7*), studies of gas-sparged bubble contactors have been directed primarily to biochemical applications such as fermentation and waste oxidation, wherein gas mass rates are generally low, in the range below 20 lbs./hr.-sq. ft. Additionally, there have been extensive studies of mechanically agitated bubble contactors, as well as a number of detailed examinations of the mechanics of single-bubble generation. However, the mechanics of bubble-swarm generation at high gas rates are unique, and the dynamic interaction of the two fluid phases in this latter instance defines a problem area that has not received the experimental attention it merits. This research therefore had its origin in the fact that the controlling parameters for an unstirred gas-sparged bubble contactor had not been previously investigated over the higher range of gas flow rates of intrinsic commercial and practical interest. This range was considered to be 25 to 300 lb./hr.-sq. ft. mass rate which corresponded to a superficial linear gas velocity range of 0.09 to 1.10 ft./sec.

The commercial scale up problem dictated mass transfer experiments in which the liquid-phase resistance controlled. The catalyzed air oxidation of sodium sulfite solution was chosen as the most applicable test system, despite reported controversy over the magnitudes of its composite gas- and liquid-phase resistances; the various literature opinions on this point have recently been reviewed by Yoshida et al. (*10*). In the present work, the sulfite test system was found to match the commercial solution in its response to gas flow and other system physical parameters, so that a translation of the data into composite resistance was not necessary.

EXPERIMENTAL APPARATUS AND PROCEDURE

The absorption studies were conducted mainly in a 4-in. diameter Pyrex pipe section, 5 ft. high. Limited supplementary determinations were made in a 3-in. diameter, 2-liter cylindrical graduate. The mechanics of bubble-swarm contacting were examined visually and by means of motion pictures in both the 4-in. and a larger 6-in. diameter Pyrex column.

The 4-in. column had five side outlets spaced in a vertical row, 13 in. between centers and 4 in. from each end, through which hypodermic syringe needles could be inserted for sampling. Air was dispersed by a four-arm sparger, each arm containing one 0.147-in. orifice facing downward at midradius, 4 in. from the column floor. The 6-in. column was equipped with a similar sparger with 0.187-in. orifices located 2 in. above the bottom flange. The gas disperser for the 3-in. reactor consisted simply of a 6-mm. glass dip tube (0.154-in. orifice), with the tip ¼ in. above the cylinder bottom.

The procedure followed was similar to that described by Cooper, Fernstrom, and Miller (*2*). Modifications of the procedure were as follows. Sodium sulfite solution was made up to approximately 1.0 N in a 5-gal. reservior, and sufficient copper sulfate was added to give a Cu^{++} concentration of 10^{-3} M. The pH of this solution was found to be about 9.0, and the alkalinity caused a small but definite amount of foaming on subsequent aeration. A more immediate effect of introducing this solution into the reaction column was the rapid electrolytic deposition of copper on the iron sparger, an effect also noted by Elsworth, Williams, and Harris-Smith (*4*). These latter investigators were successful in preventing copper deposition by painting their vessel with graphitic paint or high-melting grease. In the present study, oil-based paints were found to radically inhibit oxidation performance, a phenomenon which led to a separate investigation of mass transfer poisoning reported in Part II. A fairly effective and noninhibiting solution to the plating problem was found to be a sprayed acrylic coating.

In addition to their foaming tendency, sulfite solutions of pH = 9.0 had poor storage stability, and extensive precipitation was sometimes obtained even in nitrogen-blanketed storage. Therefore, after a few series of runs had been made, the pH was adjusted to the 7.0 to 7.2 range by the addition of 50 ml. of concentrated sulfuric acid to the initial 5-gal. solution batch. With this adjusted pH, the solution was stable, did not foam, and gave reproducible oxidation results down to a sulfite normality of 0.3 N.

Consecutive runs were made on each column batch of solution to a lower sulfite normality limit of 0.3 N. Operation below 0.3 N was avoided because pH dropped off sharply, the solution became cloudy with a green precipitate, and sulfur dioxide was evolved. Run lengths varied from 15 to 90 min., depending on oxidation rate and normality. It should be noted that the sulfite normality range of 0.3 to 1.0 N corresponded to that covered by Cooper, Fernstrom, and Miller (*2*) and is much greater than the 0.1 to 0.2 N range used by Yoshida et al. (*10*) in an investigation of stirred contactors.

Samples of approximately 25 ml. were taken by means of nitrogen flushed hypodermic syringes transferred to nitrogen-blanketed burettes and the sulfite concentration determined by standard analytical procedures (*9*). All samples were taken in

W. J. Braulick is with Esso International, Inc., New York, New York. J. R. Fair is with the Monsanto Company, St. Louis, Missouri. B. J. Lerner is a Consulting Engineer, Pittsburgh, Pennsylvania.

duplicate, and check analyses were made by two individual operators.

Gas holdup measurements were made in terms of the fluid head change as metered by an inclined CCl_4 manometer.

VISUAL OBSERVATIONS

Because certain observable changes in gas-liquid interaction in a sparged column correspond to significant changes in mass transfer behavior, it is of value to review briefly some of the more important visual observations prior to a discussion of the mass transfer results. Frame-by-frame study of motion picture films taken at 64 frames/sec. of the 6-in. contactor in operation provided the basic qualitative data on flow mechanism and phase interaction.

Air-Water System

At flow rates in the 6-in. column corresponding to superficial mass velocities G_o below 8.5 lb./hr.-sq. ft., near-spherical bubbles of ½-in. diameter were formed and ascended without distortion or coalescence at their free-rise velocities. As G_o was increased from 8.5 to 25, bubble size increased to about an inch in diameter, with an accompanying increase in bubble rise velocity. In this period of stable single-bubble formation, bubble size and formation frequency are determined primarily by the orifice size and system properties (*3*). At approximately 25 lb./hr.-sq. ft., a rapid and distinct transition in flow behavior occurred which appeared to have a rather simple starting point. This transition apparently corresponds to the point at which gas is being injected into the liquid column at a rate exceeding the capacity of the normal 1-in. bubbles to transport the gas from the sparger. The introduction of gas at a rate in excess of stable single-bubble transport capacity results in bubble coalescence at the sparger, yielding bubbles of 3 to 4 in. in diameter whose formation triggers a turbulence sequence.

The large primary bubbles resulting from initial coalescence possess exceptionally high rise velocities and generate intense local liquid turbulence in their wakes. Successive primary bubbles thus pass through a field of well-developed liquid turbulence which causes peripheral shear and disintegration of the primary bubble to yield a secondary small-bubble group with a mean diameter of from 1/10 to 1/4-in. However, the liquid turbulence which serves to break down the primary bubbles also brings about contact and recoalescence of residual or subdivided primary bubbles of 1 to 2 in. in diameter, thus reforming bubbles of the initial primary size throughout the column. With increasing flow above the transition region, the frequency of primary coalesced bubble formation increases, as does the intensity of liquid turbulence and the rate of shear formation of the secondary bubble group. This cyclic interaction behavior leads to the bubble distribution pattern shown in Figure 1A.

The most impressive visual feature of the sparged-gas contactor is the remarkable intensity of turbulence and backmixing generated in the liquid phase. In agreement with the observations of Ragatz and Baxter (*6*) of a deep-bed gas jet contactor, the orifice velocity of the gas had no apparent direct effect on the establishment and maintenance of contact-zone turbulence. And, as later measured by Siemes and Weiss (*8*), liquid backmixing at gas rates above the transition region is virtually complete.

A singular phenomenon which clearly delineated the phase interaction cycle outlined above was hemispheric-slug bubble generation. If the column liquid was allowed to become completely stagnant, and air was then introduced at a steady state gas rate above the transition flow rate, then the initial burst of air from the four orifices

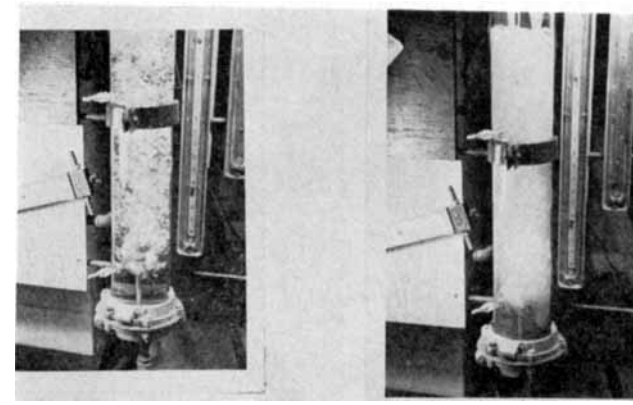

Fig. 1. Bubble dispersion in a 4-in. column. $L/D = 4.0$, $G_o = 62$ lb./hr.-sq.ft.

coalesced to form one large bubble whose diameter was equal to the diameter of the column. This air slug had a perfectly hemisphrical cap which was maintained undistorted as the bubble rose to the surface. In the wake of this initial slug of air, the normal turbulent conditions prevailed. The total coalescence of the gas injected at four different points indicates that, in a stagnant liquid field, the most stable bubble is the largest bubble that can be formed for the given gas flow. The contrast in liquid field turbulence ahead of, and behind, the hemispheric-bubble slug is a striking illustration of the mechanism by which the potential energy imparted to the liquid by gas displacement is converted to kinetic energy on bubble passage.

In a deep-bed bubble column, the primary coalesced and secondary bubbles undergo recoalescence and recombination as they rise. For depth/diameter ratios of about 7, this results in an increase in turbulence and also gas slugging in the upper portion of the column. Slugging first becomes noticeable at G_o values of 100 and slowly becomes more pronounced as G_o is increased to 300. Despite the presence of gas slugging, column operation is hydraulically stable; this may be attributed to the same phase interaction cycle operative in the other portions of the column. The more intense liquid turbulence resulting from gas expansion and/or slugging in the upper portion of the column serves to reduce greatly the residence time of any gas slug or to effect its disintegration. In either case, slugging is an extremely transient phenomenon.

Electrolyte Solutions

Visual and motion picture studies of sparged bubble swarm behavior were made of the 1.0 N sodium sulfite and other salt solutions in the 4-in. column. The significant difference in bubble dispersion in pure water and solutions of electrolytes is illustrated in Figure 1B. While the coalescence and turbulence patterns for salt solutions are the same as those observed for air dispersion in water, superimposed on these patterns in salt solutions is a fine dispersion of microscopic bubbles. Tests with sodium chloride and other salt solutions showed these swarms of minute bubbles to be characteristic of solutions of concentration greater than 0.1 M, and the extent of their formation to be a function of both concentration and gas flow rate in the 0.1 to 1.0 M range. A photograph of these small bubbles is presented in Figure 2, which shows the bubbles in the 3-in. column shortly after air flow was discontinued. Because of the nature of the solutions with which they are associated, these small bubbles are termed *ionic*.

It is important that the ionic bubbles generated in the concentrated electrolyte solutions be differentiated from the 1/10-in. diameter secondary bubbles normally generated in water or dilute solutions. For example, examination of the excellent bubble photographs of Yoshida, et al. (*10*) confirms the transition in size and population density observed for the small bubbles as agitation and concentration increased. However, Yoshida's maximum sulfite normality was 0.2 N, and his smallest bubble size is far larger than those observed in the 1.0 N solutions of this research, as shown in Figure 2. It is obvious that the interfacial contact area and residence time provided by the ionic bubble clouds are far disproportionate to the amount of gas contained in these small volumes. The ionic bubble fraction is therefore a potentially major mode of mass transfer in electrolyte solutions that would be absent in pure liquid systems.

Ionic bubble generation appeared to be associated with the areas of intense liquid turbulence, and because of their low rising velocities, these bubbles were easily carried along with the liquid eddies and served to make them visible. It was thus observed that at gas rates above the transition region of coalescence, turbulence and ionic bubble generation were depth dependent. A minimum submergence of approximately 20 in. was necessary to obtain sufficient liquid backmixing and ionic bubble formation rates to achieve ionic bubble dispersion in the lower portions of the column. The dispersion enhancement and degree of intra and interphase mixing resulting from bubble coalescence and expansion strongly suggests that a single large orifice for gas injection might be a more efficient agitation device than a series of distributed orifices.

GAS HOLDUP MEASUREMENTS

In order to place the visual observations on a quantitative basis, limited studies of gas holdup were made to determine the influence of such factors as submergence, pH, and gas flow rate. Density of the aerated mass was measured by an inclined manometer, and in this work gas holdup is a volumetric ratio defined as follows:

$$\text{Holdup} = \frac{Z_f - Z_L}{Z_L}$$

Use of the manometric method permitted studying variation of holdup with column height.

Figure 3 illustrates the effects of gas rate and submergence, diameter ratio (L/D) on gas holdup for a 1.0 N sodium sulfite solution. The data are for a solution with an adjusted pH of 7.0 in the 4-in. column at (L/D) values of 4 and 7. Although the difference between the two curves correlates with the observation that gas dispersion is depth dependent, the magnitude of this effect as measured by the gas holdup is greater than would be expected on the basis of visual observation.

The line drawn through the data for an (L/D) of 7 also fits the experimental data for an (L/D) value of 10, indicating that the submergence effect on gas holdup disappears after the initial 2 ft. of depth. However, in Figure 3, the (L/D) effect on gas holdup per unit volume of liquid persists even at the relatively low initial gas rates, which are barely in the coalescent regime. Thus, upper-region secondary coalescence and primary bubble expansion associated with $(L/D) \geq 7$ creates a turbulence reservoir which is operative throughout the coalescent region. The fact that vertical dispersion turbulence was the dominant mechanism involved in the increase in unit gas holdup at high (L/D) values was shown by measurements of the vertical holdup gradient for the 28-in. submergence. Comparison of incremental holdup data for the 0- to 13- and 13- to 26-in. submergence intervals shows that although fractional holdup was uniformly higher in the top section, the difference in unit holdup was less than half that of the differential of the 0- to 16- and 0- to 28-in. interval submergence values of Figure 3. The increased submergence thus acted to increase holdup in the lower section. This longitudinal mixing effect, coupled with the increase in turbulence with gas flow rate, yields an incremental gas holdup gain of about 30% at a G_o value of 200 for the 1-ft submergence increase from 16 to 28 in.

Comparative gas holdup determinations were also made to assess quantitatively the dispersion difference between the air-water and air-sulfite solutions shown in Figure 1. Measurements were made at an (L/D) value of 7, and these data are presented in Figure 4. The data for the 1.0 N sulfite solution of Figure 4 are for an unadjusted pH of 9.0; comparison of this line with the corresponding data of Figure 3 for pH = 7.0 shows an incremental holdup of 0.05 cu. ft. gas/cu. ft. liquid at $G_o = 200$ for the alkaline solution.

The important feature of Figure 4 is the markedly higher fractional gas content shown by the electrolyte solution as compared with water at equal mass gas flow rates; this difference amounts to a 43% increase in holdup at $G_o = 200$. From the visual studies, the sole observable difference in dispersion mechanism between the two systems was the generation of ionic bubbles in the electrolyte solution, so that the additional gas holdup must be contained in this bubble fraction. Thus, at $G_o = 200$, some 30% of the total volumetric gas holdup appears to be in these microscopic-bubble swarms which would thus possess the major portion of the total interfacial contact area.

Figure 4 indicates that although the transition to bubble coalescence occurs at about $G_o = 25$, ionic bubble gas holdup does not become significant until mass flow is increased above $G_o = 50$. Above $G_o = 50$, the difference between the two curves, that is the ionic bubble volume, is apparently linear with increasing gas flow rate. It might therefore be expected that if ionic bubble transport is the dominant transfer mode, transfer rates or coefficients should be linear with gas rate. However, while there is an inflection in the holdup curves in the 50 to 100 lb./hr.-

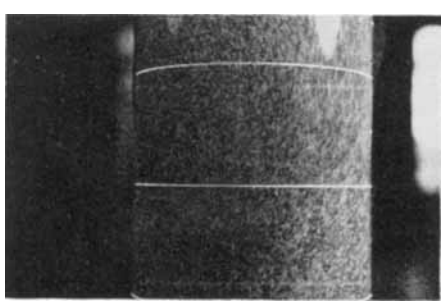

Fig. 2. Ionic bubbles in a 3-in. column (air flow discontinued).

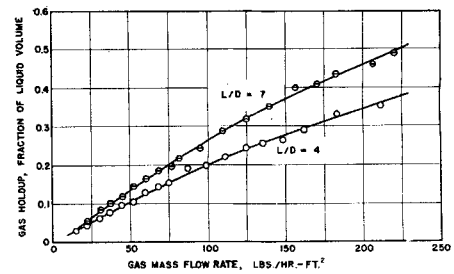

Fig. 3. Effect of submergence/diameter ratio on gas holdup (4-in. column; solution pH = 7.0).

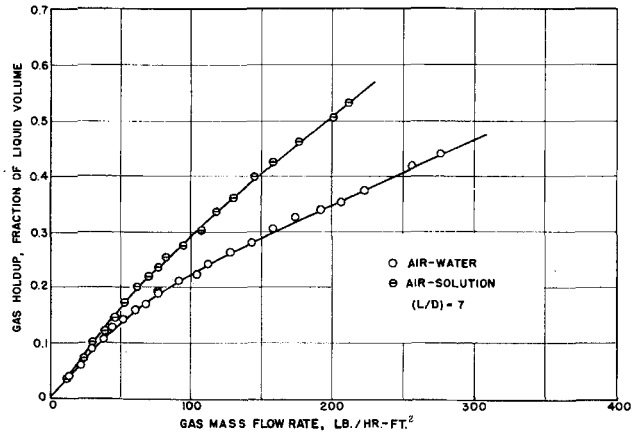

Fig. 4. Effect of liquid solution on gas holdup (4-in. column; sulfite solution pH = 9.0).

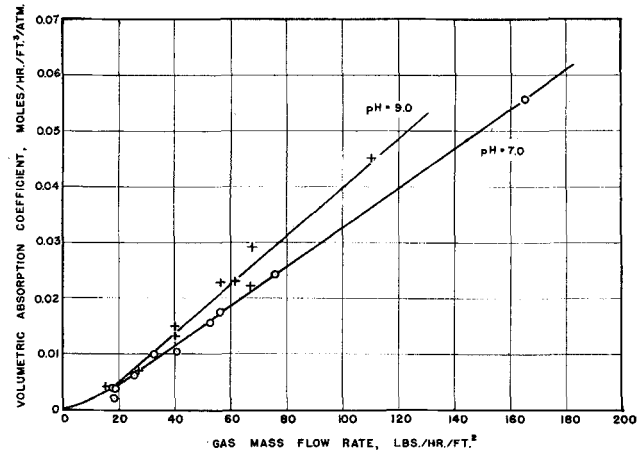

Fig. 5. Effect of solution pH on mass transfer rate (4-in. column; L/D = 4.0).

sq. ft. flow range, both water and solution show substantially straight line relationships between holdup and gas rate outside this region. Thus, linear relationships of transfer rates or coefficients with G_o would not serve to distinguish the ionic bubble transfer mode.

From a qualitative viewpoint, the ionic bubbles are small enough to behave as rigid spheres, and without internal gas circulation, their role would be different in gas-film controlled processes than in liquid-film controlled absorption. In fact, when one considers the sulfite system itself and the gas rate dependency of ionic bubble formation, it is quite possible that the transfer mechanism might change with gas flow rate and in turn explain the many conflicting interpretations of transfer resistances in this system.

MASS TRANSFER RESULTS

The quantity directly measured in sulfite oxidation experiments is the decline of sulfite concentration as a function of the time of oxidation. This quantity may be safely translated into a molar rate of oxygen absorption per unit volume of clear liquid, but further conversion into any sort of transfer coefficient necessarily involves assumptions concerning driving force and relative film resistances. As noted above, this is a somewhat uncertain procedure. Nevertheless, in order to compare the results of this research with prior literature, mass transfer rate data were converted to values of an overall volumetric transfer coefficient K_Ga based on a mean overall driving force over the column. Oxygen back pressure from the solution was assumed to be zero.

Effect of pH Adjustment

Because no previous investigator of this system had noted the initially alkaline pH and attendant storage instability of the standard sulfite-copper solution, it was necessary to establish the effect of pH adjustment on transfer coefficient. The effect is presented in Figure 5. Higher K_Ga values were obtained on the initial solution batches of pH = 9.0 than for a neutralized solution, owing to a number of factors. Most noticeable was a foam head which was generated on top of the alkaline solution; this contributed both additional interfacial contact area and gas residence time. However, the major factor, as evidenced by the comparative gas holdups, was an increase in ionic bubble content for the alkaline solution. These two factors probably account for the major portion of the approximately 25% decrease in K_Ga obtained when the pH is adjusted to 7.0. Figure 5 thus serves to establish the extent of the handicap the pH adjustment technique imposes on the K_Ga values of this investigation as compared with previously reported literature values.

Effect of Gas Rate

The preliminary holdup and visual data indicated that the prime variables governing the physical behavior of the sparged gas column were gas rate and sparger submergence. Accordingly, the sulfite oxidation runs were carried out with gas flow rate as the independent variable, with parametric values of (L/D) of 1, 2, 4, 7, and 10. The results of these runs are presented in Figures 6 and 7.

The most impressive feature of the data of Figures 6 and 7 is the magnitude of the values of the overall volumetric coefficient K_Ga. Comparison of these values with those obtained by Cooper, Fernstrom, and Miller (2) in stirred-bubble contactors shows that relatively high power consumptions gave K_Ga values of the order of 0.1 moles/hr.-cu.ft./atm. as against the 0.07 moles/hr.-cu.ft./atm. obtained for the unstirred reactor of this research at an (L/D) of 10.

Apparently, the transfer capacity level made possible by power stirring may be largely equalled in an unstirred unit through proper design and the use of high gas mass rates. However, because the agitation source in an unstirred sparged unit is the short-residence-time coalesced primary bubble, such capacity equivalence to power-stirred units is limited to systems such as air-oxidation involving once through gas passage. Additionally, with increasing (L/D) and gas rate, an economic limit would be reached at which the power required for gas compression and circulation for an unstirred reactor would equal that for operating a stirrer, unless corrosion or rotating shaft sealing problems also entered into consideration. It would appear that within these limitations there are numerous application areas for high gas load unstirred sparged contactors which have not as yet been exploited.

The linearity of K_Ga with G_o (Figures 6 and 7) is consistent with the influence of gas rate on gas holdup. The effect of submergence on K_Ga is apparent from the figures, but to obtain a more quantitative effect smoothed data from Figures 6 and 7 were cross plotted as shown in Figure 8. The equivalence of slopes enables summarizing the submergence effect in equation form:

$$K_Ga = (2.5 \times 10^{-4}G_o - 0.002)\,(L/D)^{0.3}$$

This variation of K_Ga with (L/D) to the 0.3 power compares closely to the 0.26 power variation found by Shulman and Molstad (7) for carbon dioxide desorption. It seems clear that height induced turbulence is a basic variable in the study of gas-sparged contactors.

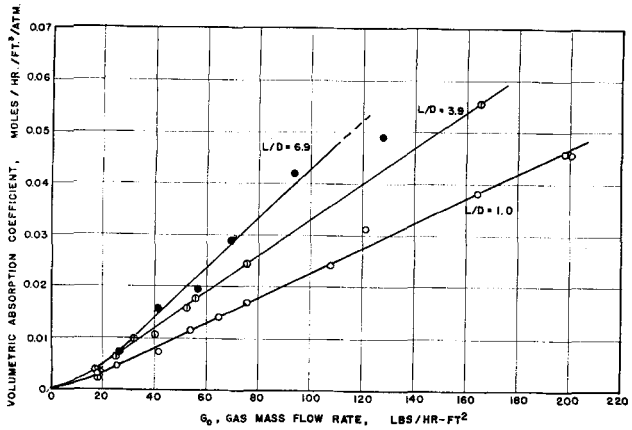

Fig. 6. Effect of submergence/diameter ratio on mass transfer rate (4-in. column; sulfite solution pH = 7.0).

The availability of K_Ga data from both the 4-in. and 3-in. diameter columns allowed the testing of mass flow rate and (L/D) ratio as applicable parameters. Transfer coefficient data for the two column diameters are plotted in Figure 9 as a function of G_o for a constant (L/D) ratio of 4. While a single line is obtained for both sets of data, the difference in submergence amounts to only 4 in., so that verification of the (L/D) ratio is only partial. On the other hand, the two sets of G_o values are based on an area ratio of 16:9, and it is apparent that superficial column velocity adequately accounts for the diameter effect in an unstirred sparged bubble column in this size range. This behavior further indicates the equivalence of agitation level achieved in a simple sparged contactor and a mechanically agitated reactor, inasmuch as the superficial gas velocity has previously been shown to be the proper correlating variable for stirred units (2).

The gas rates in this work are higher than those previously reported for sparged contactors, and comparisons with other mass transfer data in the literature are not possible. The related studies of Shulman and Molstad (7) in a 4-in. sparged unit covered gas rates only up to 75 lb./hr.-sq.ft., utilized liquid counterflow, and where concerned with the transfer of carbon dioxide in water. Perhaps the most closely comparable work is that sponsored by the American Institute of Chemical Engineers Research Committee in connection with distillation column design. Although the submergences were low and the contacting mechanisms of deep beds largely absent, the gas rates were high and in fact extended considerably beyond those of this work.

Comparisons between the American Institute of Chemical Engineers work and this present work are shown in Figure 10. The American Institute of Chemical Engineers data (1) are for oxygen desorption from water, with reported k_La values converted by the expression

$$K_Ga = k_La/H$$

where the Henry's law coefficient at 25°C. was taken as 4.25×10^5 atm./mole fraction. The very good agreement with shallow bed results $(L/D = 1.0)$ of this work is apparent. Whether this is fortuitous is not clear; however, it may be noted that on the basis of individual cap vapor fields, the (L/D) for the American Institute of Chemical Engineers work was essentially 1.0.

Projection of the linear portions of the curves of Figures 5, 6, and 7 shows that they do not originate at the origin but rather indicate a transition at a G_o value of about 20. This is, of course, in accord with the visually observed change in bubble mechanism to coalescence at this point. It is of interest that this transition is not reflected in the holdup data of Figure 4. While no runs were made in the precoalescence region in this research, Yoshida, et al. (10) have presented data for k_La as a function of gas rate for sulfite solution oxidation in an unstirred bubble reactor in the 0 to 20 lb./hr.-sq.ft. region. The slope of the k_La vs. G_o lines on the original log-log plot is substantially 1.0, so that transfer coefficient is directly proportional to gas rate in both the precoalescent and coalescent regimes. However, there is a substantial differ-

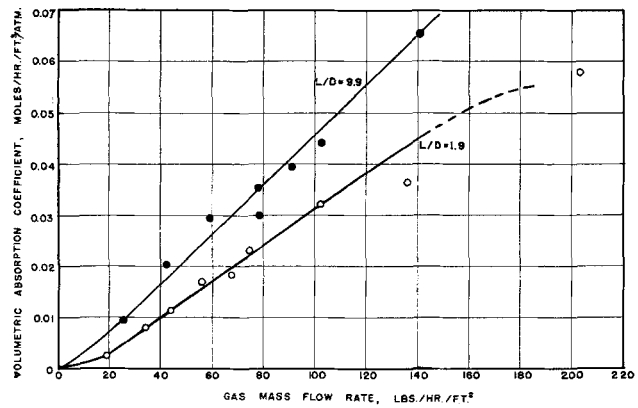

Fig. 7. Effect of submergence/diameter ratio on mass transfer rate (4-in. column; sulfite solution pH = 7.0).

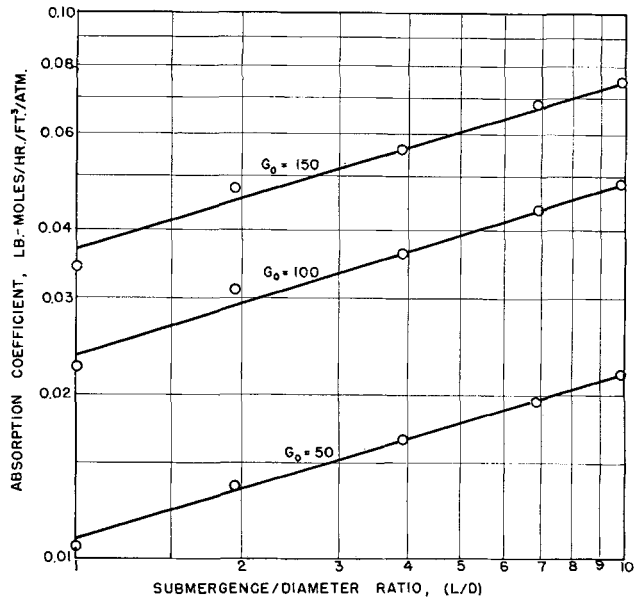

Fig. 8. Effect of submergence on mass transfer (4-in. column; sulfite solution pH = 7.0).

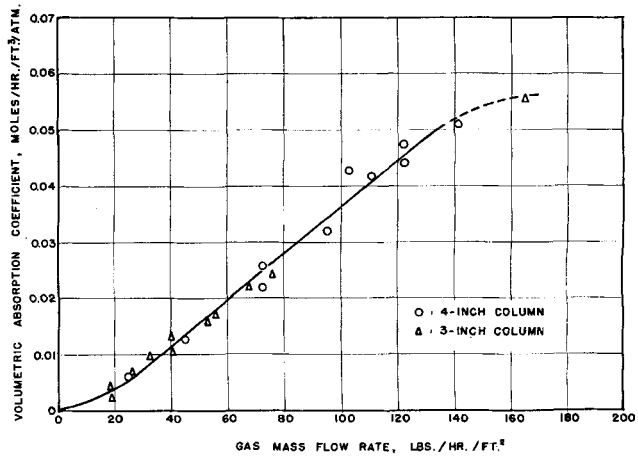

Fig. 9. Effect of column diameter on mass transfer (L/D = 4.0; sulfite solution pH = 7.0).

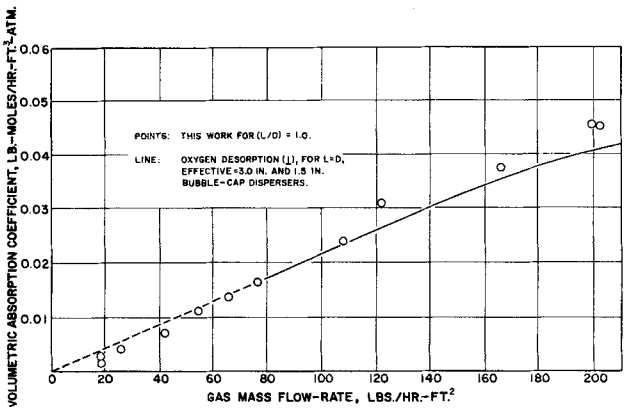

Fig. 10. Comparison of mass transfer for oxygen absorption and desorption.

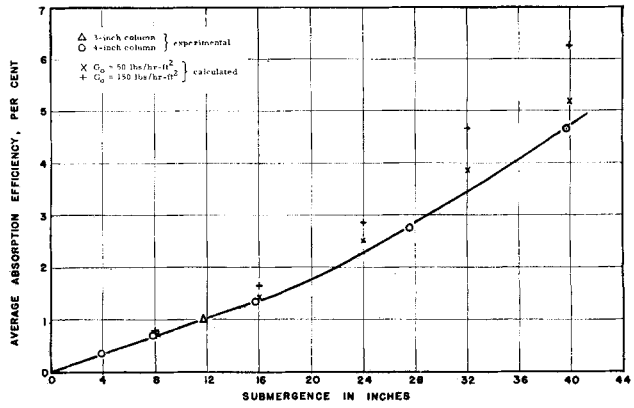

Fig. 11. Effect of submergence on absorption efficiency.

ence in the order of magnitudes of the coefficients associated with the two flow regimes, as is evident in Figures 6 and 7.

Absorption Efficiency

While the present data show that the transfer capacity of the unstirred sparged contactor is virtually equal to that attainable in a mechanically agitated unit, the comparative absorption efficiencies must also be considered. For the data of Figures 6 and 7, the fraction of the inlet oxygen that was absorbed in passage through the column, expressed as an oxygen efficiency E_{oG}, varied from 0.5 to 5% and was found to be completely independent of K_Ga. Additionally, plots of efficiency against gas rate showed no effect of G_o above a flow rate of 50 lb./hr.-sq.ft. Although these efficiencies are of the same order of magnitude as many of the values obtained by Cooper, Fernstrom, and Miller (2) for a stirred laboratory contactor, they are well below the values obtained by these investigators at either very high power inputs or in plant-size equipment. It appeared likely that this effect of equipment scale for stirred contactors was primarily a residence time phenomenon, which might also be evident in the unstirred reactor as a submergence effect.

The efficienecy may be defined in terms of transfer units as

$$E_{oG} = 1 - e^{-N_{oG}}$$

where the number of transfer units is defined as

$$N_{oG} = \frac{K_Ga\pi Z_f}{G_M}$$

Substitution of K_Ga and Z_f (from holdup) data of Figures 3, 6, and 7 in this equation shows that for a given submergence N_{oG} (and hence E_{oG}) should be slightly dependent on gas rate. The experimentally determined curve relating E_{oG} to submergence is shown in Figure 11, and superimposed on the plot are efficiency values calculated from observed values of K_Ga and Z_f. The agreement between calculated and experimental efficiencies is reasonably good, but at higher submergences the simplified model obviously does not apply.

The change in slope of the efficiency curve at submergences greater than 20 in. reflects changes in liquid recirculation patterns. Apparently, the increase in effective residence time at the greater depth is due to increased intensity of backmixing of smaller bubbles.

The constancy of gas holdup for (L/D) values of 7 and 10, and the apparent increase in residence time in Figure 10 for this submergence range, is evidence that the average bubble contact time is not a simple function of gas velocity and holdup, as has been suggested by Foust, Mack, and Rushton (5). In view of the changing bubble population with gas rate and the different susceptibilities of primary and ionic bubble sizes to downward eddy currents, it is doubtful that a simplified (calculated) average residence time would be consistently applicable over the entire flow range.

The availability of sampling taps at 13-in. intervals of depth in the 4-in. reactor permitted the simultaneous withdrawal of samples to check the extent of vertical mixing. Comparisons were obviously limited to (L/D) values of 7 or above. Samples taken for a number of runs showed that in no case was there a detectable difference in unreacted sulfite concentration between vertical stations. It is therefore evident that longitudinal mixing is highly effective and yields a perfectly mixed liquid phase at high (L/D) ratios. Viewed as a mass transfer device, the deep-bed sparged bubble contactor would thus yield a maximum of one equilibrium stage. In many instances of catalytic reaction, however, one equilibrium stage would correspond to complete conversion, so that the sparged bubble reactor definitely merits consideration as a simple and economic reactor type.

CONCLUSIONS

These studies of deep-bed gas-sparged bubble columns have delineated contacting mechanisms and have provided holdup and mass transfer data useful for design. The range of gas rates has been broad enough to cover most commercial applications of the equipment type.

At low gas rates the mechanics of bubble swarms are functions of disperser design and free rise velocities. At intermediate gas rates, coalescence into larger bubbles occurs, with secondary smaller bubbles resulting from the shearing action of liquid turbulence. At high gas rates, slugging develops, particularly at submergence/diameter ratios of 7.0 or higher.

In electrolyte solutions, particularly those with high submergence values, large numbers of very small ionic bubbles appear. These bubbles tend to be circulated with the liquid and contribute significantly to mass transfer because of their high interfacial area and long residence time.

Gas holdup and mass transfer were found to increase with gas rate and with submergence/diameter ratio. The mass transfer characteristics of the gas-sparged bubble column were found to be equivalent to those of stirred vessels. Also, at gas rates in the turbulent contacting regimes, essentially complete backmixing of the liquid was observed.

ACKNOWLEDGMENT

The experimental work, part of which was obtained by W. J. Braulick for his Master's Thesis, was carried out in the laboratories of the Department of Chemical Engineering of the Uni-

versity of Texas. Thanks are due to the staff of that institution, as well as to Drs. H. E. Morris and W. H. Lane of Monsanto's Texas Division, for their help and comments.

NOTATION

D = column diameter, in. or ft.
E_{OG} = absorption efficiency = $(y_1 - y_2)/y_1$
G_o = superficial gas mass velocity, lb./hr.-sq.ft.
G_M = superficial gas molar velocity, lb.-moles/hr.-sq.ft.
H = Henry's law constant, atm./mole fraction
k_La = volumetric liquid phase mass transfer coefficient, lb.-moles/hr.-cu.ft.-mole fraction
K_Ga = volumetric overall mass transfer coefficient based on gas phase, lb.-moles/hr.-cu.ft.-atm.
L = nongas flow submergence, in. or ft. of liquid
L/D = submergence/diameter ratio
N_{OG} = number of overall transfer units based on gas phase, dimensionless
y = mole fraction of oxygen in air
Z_f = observed height of aerated mass, in. or ft.
Z_L = equivalent height of clear liquid (also L), in. or ft.
π = total pressure, atm.

LITERATURE CITED

1. American Institute of Chemical Engineers, "Tray Efficiencies in Distillation Columns," Fourth Annual Progress Report, pp. 9 and 45, New York (June 30, 1956).
2. Cooper, C. M., G. A. Fernstrom, and S. A. Miller, *Ind. Eng. Chem.*, **36**, 504 (1944).
3. Davidson, L., and E. H. Amick, *A.I.Ch.E. Journal*, **2**, 337 (1956).
4. Elsworth, R., V. Williams, and R. Harris-Smith, *J. Appl. Chem.*, **7**, 269 (1957).
5. Foust, H. C., D. E. Mack, and J. H. Rushton, *Ind. Eng. Chem.*, **36**, 517 (1944).
6. Ragatz, E. G., and H. A. Baxter, *Oil and Gas J.*, **54**, No. 50, p. 158 (April 16, 1956).
7. Shulman, H. L., and M. C. Molstad, *Ind. Eng. Chem.*, **42**, 1048 (1950).
8. Siemes, W., and W. Weiss, *Chem.-Ing.-Tech.*, **29**, 727 (1957).
9. Willard, H. H., and N. H. Furman, "Elementary Quantitative Analysis," Van Nostrand, New York (1948).
10. Yoshida, F., A. Ikeda, S. Imakawa, and Y. Miura, *Ind. Eng. Chem.*, **52**, 435 (1960).

Manuscript received May 22, 1963; revision received August 17, 1964; paper accepted August 19, 1964. Paper presented at A.I.Ch.E. Buffalo meeting.

Kinetics of the Heterogeneous Decomposition of Iron Pentacarbonyl

HERBERT E. CARLTON and JOSEPH H. OXLEY

Battelle Memorial Institute, Columbus, Ohio

The decomposition of iron pentacarbonyl at pressures between one and 400 Torr was studied from 120° to 300°C. Up to about 200°C. the rate was primarily limited by surface kinetics of adsorbed carbonyl. Gas phase diffusional resistances were controlling at higher temperatures. In the kinetically controlled region the deposition rate was correlated by a Langmuir type of equation. Corrections for diffusion resistances in the kinetic region and kinetic resistances in the diffusion region were found to be appreciable.

A study of the thermal decomposition of iron pentacarbonyl was undertaken as part of a broad investigation of the basic mechanisms during the vapor deposition of solid materials. Iron pentacarbonyl was one reactant chosen for studying mass transfer characteristics. It decomposes in accordance with the overall equation:

$$Fe(CO)_5 \rightarrow Fe + 5CO \qquad (1)$$

The decomposition results in an unusually high molar ratio of products to reactants which should severely test the Stefan-Maxwell diffusion equations and mass transfer analogies, and the carbonyl decomposes at a low temperature which simplifies experimental techniques. Iron carbonyl is also especially suited for a study of combined kinetics and diffusion, since the decomposition is highly